Proceedings of the 2nd International IEEE EMBS
Conference on Neural Engineering
Arlington, Virginia · March 16 - 19, 2005

A High Performance Neurally-Controlled Cursor Positioning System

Gopal Santhanam[1], Stephen I. Ryu[1,2], Byron M. Yu[1], Afsheen Afshar[1,3], and Krishna V. Shenoy[1,4]
[1]Department of Electrical Engineering, Stanford University, Stanford, CA 94305, USA
[2]Department of Neurosurgery, [3]Stanford University School of Medicine, Stanford, CA, 94305, USA
[4]Neurosciences Program, Stanford University School of Medicine, Stanford, CA, 94305, USA

Abstract— **Prior work has shown that neural activity from the primate brain can maneuver a computer cursor to specified visual targets. This cursor movement can take over a second, longer than the time for an arm reach to the same location. We asked if this acquisition time could be reduced, thereby increasing the number of targets that could be hit per second. We implemented a system that positions a prosthetic cursor at discrete locations, based on pre-movement neural activity in rhesus monkeys. Using a delayed center-out reaching task with several different target layouts, neural activity was simultaneously recorded from an electrode array implanted in the dorsal pre-motor cortex. We designed a target prediction algorithm based on maximum-likelihood models (using Gaussian or Poisson distributions) to decode the upcoming reach target in real-time. During cursor trials, the algorithm predicted the most likely reach target using 50-275 ms of delay activity starting at least 150 ms after target onset. If the target prediction was correct, a cursor was positioned and the monkey received a reward. The performance of the system was evaluated based on the accuracy of decoded targets and speed at which targets were decoded, both of which were consolidated with an information theoretic analysis. The maximum average sustained rate of target acquisition was 4.3 targets per second obtained with a 2 target layout and 50 ms of delay activity. The maximum information transfer rate calculated for the system was 6.5 bps obtained with an 8 target layout and 100 ms of delay activity.**

Keywords— **brain-machine interface, motor control, pre-motor cortex, information theory, neural prostheses.**

I. INTRODUCTION

THE concept that neural activity can be used to control external devices, such as artificial arms, dates back to at least the late 1960s [1], [2]. This idea has been reexamined in recent years in rats [3], monkeys [4]–[7], and humans [8], [9]. These current motor prosthetic systems typically take a second or more to move a prosthetic effector (either a cursor on a computer screen or a robotic arm) to hit a target.

Such motor prostheses can be viewed as communication prostheses if each target location is likened, for example, to a key on a keyboard. This strategy has been successfully employed with electroencephalogram (EEG) driven systems [10], [11], electrocorticographic (ECoG) driven systems [12], and cortically-driven [8], [13] and subcortically-driven systems [14], and has allowed ALS "locked in" patients to type messages. Although clearly successful at one level, the performance of these systems falls short of providing a high throughput communication device. Human systems can accurately type just a few letters per minute ($\leq$0.5 bits/s equivalent; [10]), and until now monkey-based systems using activity from tens or hundreds of neurons can accurately hit targets only once every second or more ($\leq$1.5 bits/s equivalent; [15]).

Communication prostheses are not obliged to move the cursor along a continuous path in order to strike the target, but rather they can simply position the cursor directly on the target. Aside from the obvious benefits of reducing the space of parameters to extract (e.g., direction and speed at each instant of time), there is the additional benefit of removing the requirement for visual feedback during the estimation process. Visual feedback introduces many tens of milliseconds of latency into the feedback controller, thus limiting the speed with which corrective movements can be made.

With this design philosophy in mind, we investigated the neural activity in the dorsal pre-motor cortex (PMd) to explore how it might best provide *fast* and *accurate* targeting information. Here, we report the design criteria that we considered in conjunction with our experimentally-observed performance results.

II. METHODS

We recently designed and conducted a series of experiments to begin to explore the fundamental performance limits of communication prostheses [16], [17]. We trained two rhesus monkeys (G and H) to perform delayed center-out reaches as shown in Fig. 1(A). For each monkey, we simultaneously recorded neural activity from single- (typically many 10s) and multi- (typically $>$100) neural units from a 96-channel electrode array implanted in arm representation of PMd, contralateral to the movement limb (left arm, monkey G; right arm, monkey H). We used a previously reported recording setup [18]. We presented various target configurations on the screen. These included layouts with 2, 4, 8, or 16 directions and 6–12 cm radial distance.

Trials begin when the monkey fixates a magenta cross and touches a central yellow square. Following a touch hold time (200–400 ms), a visual target cue appears on the screen. After a pseudo-randomized (200–1000 ms) delay period, a

---

This work was supported by the NDSEG Fellowship (G.S. and B.M.Y.), the NSF Graduate Research Fellowship (G.S. and B.M.Y.), the Christopher Reeve Paralysis Foundation (S.I.R. and K.V.S.), Medical Scientist Training Program (A.A.) and the following awards to K.V.S.: the NSF Center for Neuromorphic Systems Engineering at Caltech, ONR, Whitaker Foundation, Center for Integrated Systems at Stanford, Sloan Foundation, and Burroughs Wellcome Fund Career Award in the Biomedical Sciences. Please address correspondences to `gopals@stanford.edu`.

"go" cue (fixation and central touch targets are extinguished) indicates that a reach should be made to the target. Neither hand nor eye were allowed to move until this go cue was presented. Subsequent to a brief reaction time, the reach is executed, the target is held (200 ms), and a juice reward is delivered. An inter-trial interval is enforced before starting the next trial.

Monkeys perform approximately 25–50 interleaved trials for each reach target during the training phase of the experiment. We collected data from the delay period epoch (a length of T_{int} starting T_{skip} after target presentation) and, for each target location, the distribution of spike counts for each trial was modeled using either a Poisson or multivariate Gaussian distribution. We used maximum-likelihood methods to choose the most probable reach target based on neural data from the same time window chosen for the model training phase. For all offline analyses, we estimated the average accuracy of the target estimator using leave-one-out cross-validation techniques with the trials in our training set. For online experiments, we had two separate blocks of trials, one for training and one for testing.

A. Skip Time

The first timing parameter we assessed relates to the time delay between when a visual target is presented on the screen and when PMd neurons have established a reach plan. This time, T_{skip}, includes (1) the time for visual information to be processed by regions in the central nervous system and relayed to PMd (∼50–70 ms), (2) the time needed, by the brain, to select among the newly seen potential reach targets and (3) the time needed, by the brain, to form a reach plan. Until these three processes are complete, the plan is still ill-formed and would inject noise into the target estimator. Hence, skipping a certain interval immediately following the cue presentation can improve the overall accuracy of the system. We can gain insight into these processes by analyzing the data offline, sliding a short estimation window after cue onset time and assessing when the average accuracy of the target estimator begins to plateau.

Another critical question is whether the neural activity measured during the delay period is primarily related to a reach plan or is merely a by-product of the visually cued stimulus. It is imperative that the former be true if we wish to draw an analogy between our performance measurements and a human prosthetic system — a clinical system must rely on internally generated target plans as opposed to cued stimuli. While we decided to use the one target task in the prosthetic cursor task, we sought to establish a T_{skip} that was relatively conservative. We repeated our initial T_{skip} analysis on data from a "distractor" delayed reach task. This task presents all of the eight possible reach locations on every trial, but only one is colored yellow while the rest are colored green. (PMd neurons are neither known nor thought to be color selective.) The monkey was trained to reach for the yellow target following the delay period. For each configuration, the estimator accuracy was computed by using the sliding window analysis. The estimation performance in the distractor task was compared to that in the standard one target task within the same experiment (interleaved trials). Placing T_{skip} at the time where these two performance curves converge assuages the concerns regarding visually cued stimuli; the distractor task presents eight visual targets so purely visual information cannot explain this performance result.

For monkey H, the distractor task analysis yielded a larger T_{skip} than for monkey G. We hypothesized that this monkey was serially searching through all eight stimuli to find the yellow target instead of experiencing a pop-out effect. In order to test this explanation, we changed the color of the distractors to blue, providing easier discriminability between the reach target and the distractors. All targets were presented isoluminent.

B. Integration Time

The integration time, T_{int}, refers to the window over which spiking counts are calculated for target estimation. Given that the spiking of neurons is a stochastic process, one can obtain a more accurate estimate of the underlying mean spiking count (and thus a more accurate estimate of the target) if longer windows are used (assuming that firing rates are relatively constants). As such, there is a fundamental tradeoff in the choice of T_{int}: a larger T_{int} increases single-trial accuracy but decreases the number of targets estimated per second. For example, one can choose T_{int} based on the minimum value that yields a desired single-trial accuracy value. We fixed T_{skip} to a value determined from earlier analyses and simulated different T_{int} times offline to understand the impact of integration time on accuracy.

C. Information Theoretic Analysis

Different target layouts require different T_{int} times to yield a desired accuracy. Alternatively, T_{int} could be chosen to be the value which maximizes the information transmission rate, a quantity measured in bits per second (bps). The information transmission rate is given by the well-known channel capacity introduced by Shannon [20]. The channel capacity is the quantity that maximizes the mutual information between the target presented and the target estimated and it provides a theoretical upper-bound on the amount of information that can be transmitted through a communication system, based solely on the error pattern of the communication channel. In our experimental setup, the communication system consists of a source (PMd) planning a reach to a given target (the communication symbol to be transmitted). The receiver (our prosthetic system) decodes the neural activity and produces an estimate of which symbol was transmitted (our estimate of the reach target).

To estimate the information transmission rates afforded by our prosthetic system, we calculated the information capacity using the Blahut-Arimoto algorithm [21].

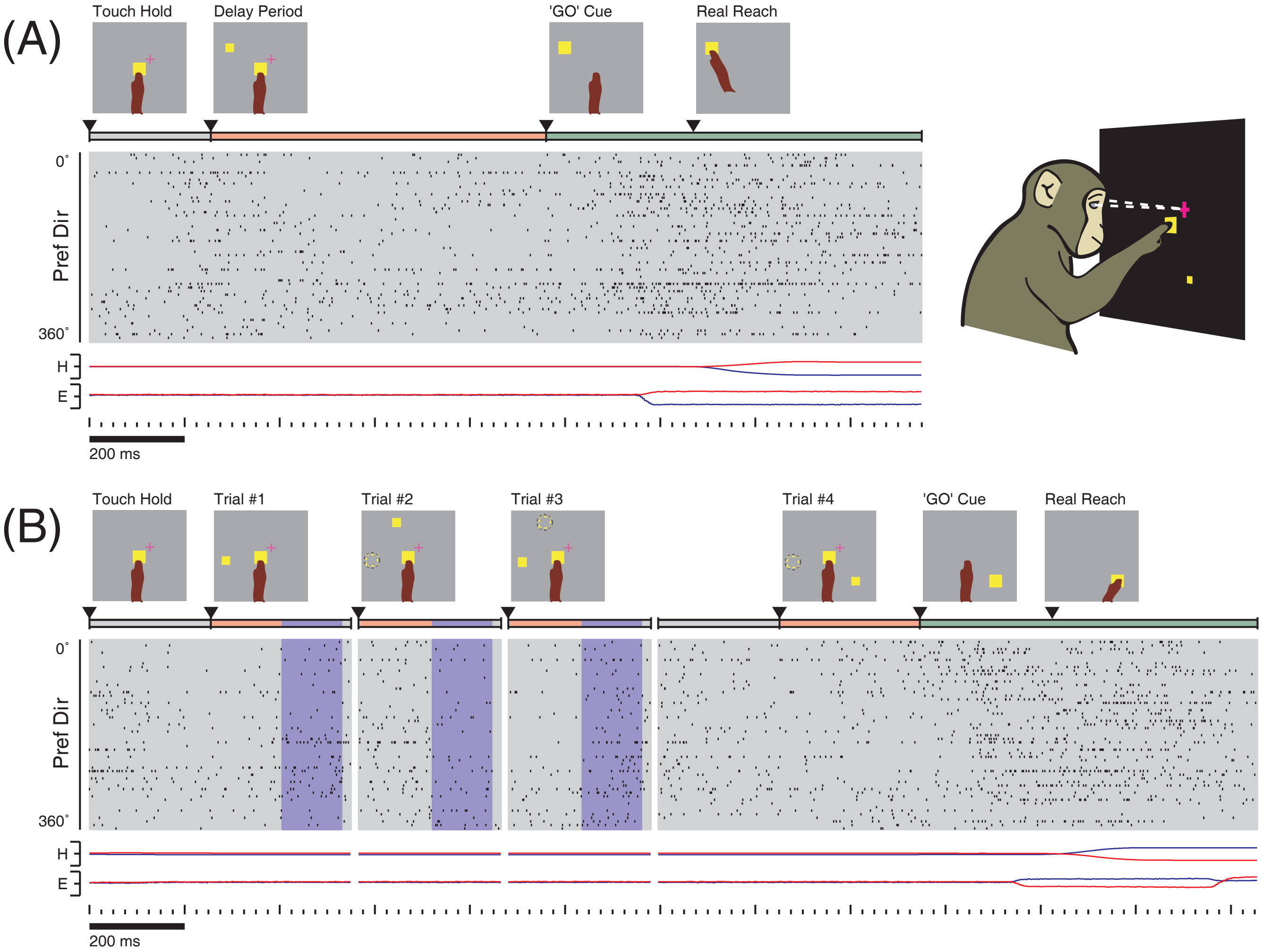

Fig. 1. Task description with data from experiment `H20041106`. **(A)** Standard reach trial. Selected neural units (based on tuning and depth of modulation) are shown in raster form, sorted by preferred angular tuning direction [19] during the delay period (pink shading on timeline). Hand and eye position traces are shown, where blue corresponds to the horizontal coordinate, red to the vertical coordinate. **(B)** Chain of three successful prosthetic cursor trials followed by a standard reach trial. Neural activity was integrated during the purple shaded segment of the delay period and used to estimate the reach target location. After a small processing delay of ∼50 ms a prosthetic cursor is briefly rendered and a new target is displayed. (This rapid display of the prosthetic cursor along with the rapid extinguishing of the original reach target are designated by dotted lines as opposed to solid lines.) Note that the eye and hand were held constant during the cursor trials. This, along with measurements of EMG activity in monkey G, highly suggest that the target estimator is not using directionally tuned movement activity.

D. Online Feedback

While offline experiments can give insight into system performance, these analyses are often performed on trials with long delay periods and long inter-trial intervals. In these simulations, one can run the target estimator with very short $T_{skip}$and T_{int}times and an estimate can be generated very soon after the start of a trial. However, the next target is only displayed several 100s of milliseconds later. Hence, the offline experiments as designed cannot accurately assess a *sustained* information rate. It is quite possible that if targets are displayed rapidly — immediately after the preceding trial's reach target has been estimated — that the performance of the system can be significantly compromised. For example, the reach plan region of the brain may simply not be able to keep up with such a fast pace of target presentation.

To design and test performance, we built a real-time system that positions the prosthetic cursor at discrete locations, akin to the location of keys on a keyboard, based on the delay-period neural activity. Training trials were collected to build a model and the subsequent trials were processed by the target estimator. During each trial, the target was estimated and this estimate was rendered back to the monkey as a small circle. If the estimate was correct, a subsequent target was cued with very little delay. Real reaches were interspersed to keep the animal engaged in the task. Fig. 1(B) shows an example of a consecutive sequence of three prosthetic cursor trials followed by a standard physical reach trial. It is unlikely that the monkey

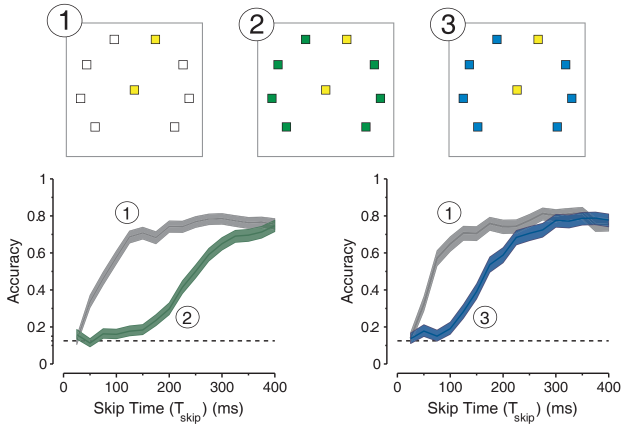

Fig. 2. Skip time results. Top row: schematics of (1) standard task, (2) yellow-green distractor task, (3) yellow-blue distractor task. Bottom row: left panel shows results from yellow-green experiment `H20041117` and right panel corresponds to yellow-blue experiment `H20041201`. For each experiment, the gray curves show performance for the standard one target delayed reach task, while the colored curves correspond to the distractor task. The decode performance is assessed through the average probability of the correct reach target (1 of 8). The integration time for this analysis is 50 ms. Shading reflects 95% confidence intervals. Dashed lines represent chance level of 12.5%.

cognitively appreciated the meaning of the prosthetic cursor given the brevity of its presentation, but our behavioral control software used the correctness of each estimate to dictate the timing and reward of each trial. As such, our system was operating under feedback control.

We tested different trial lengths and target configurations to assess the average accuracy of our target estimator as well as the information transfer rate.

III. RESULTS

A. Skip Time

Fig. 2 shows the probability of predicting the correct reach target (which 1 of 8) versus the skip time in monkey H. The gray curve shows that at time 150 ms (estimation window spans 150–200 ms) the true reach target could be predicted ∼70% of the time (leave one out cross validated simulations). By 300 ms (estimation window 300–350 ms) the result was closer to 80%, reflecting a slight increase in target-predictive information.

For the yellow-green distractor task, the green curve starts near chance level and merges with the single target task by ∼400 ms. At this time, PMd definitively reflects a reach plan rather than merely the location of the visual target. For the yellow-blue distractor task, the distractor performance merges with the single target performance by ∼250 ms. This large difference between the two distractor tasks suggests that the difficulty of the task can greatly influence the speed at which plans are formed. Finally, for larger integration windows as we use in online experiments, the performance curves for each configuration (distractor vs. single) converge at earlier values of T_{skip}. As a result, we chose the skip time equal to 150 ms.

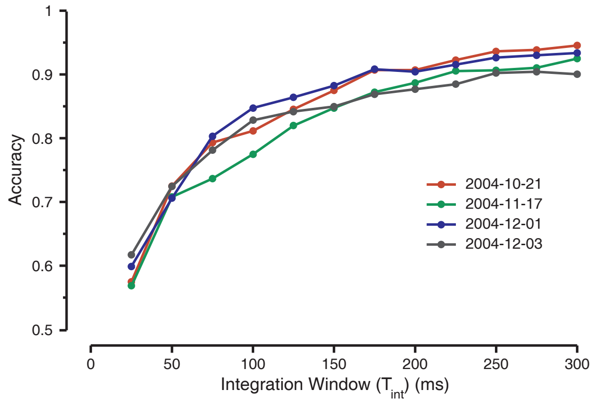

Fig. 3. Integration time results. Performance versus integration time is plotted for four different experiment days with monkey H. T_{skip} = 150 ms was used for all simulations. Chance level is 12.5%.

In monkey G the yellow-green distractor experiment showed convergence at ∼250 ms for 50 ms integration windows; hence, the yellow-blue experiment was not performed.

B. Integration Time

Fig. 3 shows the probability of predicting the correct reach target (which 1 of 8) versus the integration time used by the target estimator. Despite the slight experiment-to-experiment variability in the estimates, the performance consistently saturates around T_{int} = 200 ms. The accuracy is around 85–90% at this point. Longer T_{int} times do not yield much better accuracy, but do compromise the speed at which targets can be decoded. These results were consistent across both monkeys.

C. Information Transfer Rates

Fig. 4 shows the information transfer rate versus trial length. As expected, the bits per trial generally increases with increasing trial length since longer trials allow for larger integration windows and increased accuracy. However, the plot also demonstrates an interesting tradeoff in the information transfer per unit time. It is critical to keep T_{int} brief, even at the expense of accuracy. This is due to diminishing returns: beyond some optimal point, the subsequent gain in accuracy (and bits per trial) for each additional millisecond of T_{int} is so small that bps begins to decrease. The bps vs. trial length curve reveals the optimum T_{int} for maximum information transfer.

D. Online Performance

For our online experiments, performance was calculated for each experimental configuration using several hundred test trials. The maximum average sustained rate of target acquisition was 4.3 targets per second (tps) obtained with a 2 target layout, T_{skip} = 150 ms, and T_{int} = 50 ms. For this simple two target configuration we found that T_{int} = 50 ms

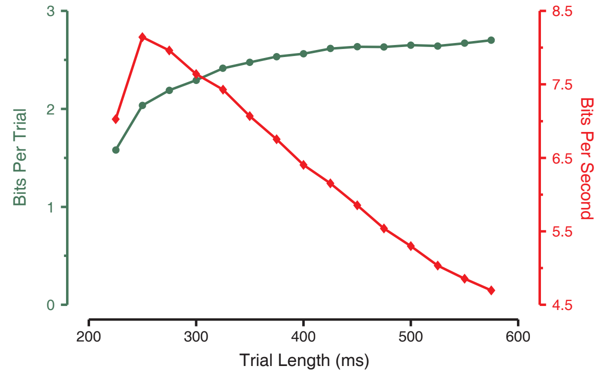

Fig. 4. Information transfer rates. Bits per trial (bpt) and bits per second (bps) were calculated offline from experiment `H20041118`. An 8 target configuration was used in the experiment. Trial length was taken to be (T_{skip}+T_{int}+50) ms with T_{skip} fixed at 150 ms and an extra 50 ms added to account for processing overhead in decoding the target, displaying the estimate, and preparing to cue the next target in real-time.

provided good accuracy (86.1%) since the classification only required binary discrimination. Table I lists the results for different target configurations for some of our fastest trial times. We present these numbers to help develop intuition before showing a more comprehensive view of our data. The 16 target data for monkey G shows particularly poor accuracy since the quality of neural recordings was deteriorating by the point that particular experiment was conducted.

TABLE I

PERFORMANCE SUMMARY FOR FASTEST EXPERIMENTS

	Targets		Performance		
	# of targets	max bits/trial (max bpt)	trials/s (tps)	accuracy (%)	bits/s (bps)
H	2	1	4.3	86.1	1.8
	4	2	3.9	73.6	3.4
	8	3	3.8	56.7	5.0
	16	4	3.5	38.7	5.6
G	2	1	3.6	84.2	1.3
	4	2	2.8	79.6	3.1
	8	3	2.8	67.5	4.9
	16	4	2.2	26.4	3.1

Each target layout can also be evaluated in terms of maximum achievable bits per trial, which is equal to $\log_2$ of the number of targets. If our system was able to achieve perfect accuracy with the 2 target layout (1 max bpt), then we would have achieved 4.3 bps information transmission rate with fastest experiment using monkey H. Achieving only 86.1% accuracy resulted in only 1.8 bps. Table I provides bps values for other target layouts.

Preliminary experiments and analyses of how accuracy and bit rate change as a function of target configuration and trial length were performed with monkey H (Fig. 5). Consistent with the trends noted in our offline study, decode performance saturated as a function of trial length (or T_{int}). Different T_{skip} times were chosen on a experiment-by-experiment basis based on the cross-validated performance of the training trials. The range for T_{skip} was 150–250 ms.

The online bit rate curves also show the existence of a peak, consistent with Fig 4. The maximum achievable bit rate was 6.5 bps for the 8 target configuration.

IV. DISCUSSION

In our effort to design a high-performance neural prosthetic system, we started by performing offline analyses to better understand the time epochs of interest. Specifically it is important to bias the system in a region where T_{skip}, T_{int}, and the target configuration are optimized for desired design specifications, whether it be accuracy, speed, or information transfer rate.

First, our T_{skip} time of at least 150 ms is consistent with previous studies showing that visual phasics in PMd neural activity typically last ∼150 ms when a visual target is flashed briefly and is not present during the memory delay period [22]. Furthermore, while the rise in performance for the distractor task is considerably slower than that of the one target task, the two curves converge around 250 ms. This presumably reflects the time consumed to identify which of the eight spots of light is the true reach target. Such a direct comparison between the two tasks allows us to avoid potential confounds and apply our results more broadly to non-cued reach plans.

Next, the analysis of T_{int} showed that accuracy begins to plateau around T_{int} times of 300 ms (or total trial times of ∼450 when T_{skip} is 150 ms). A high-speed prosthetic system should operate at speeds faster than this unless the very small gains in accuracy are absolutely necessary.

The survey of various target layouts illustrated the fundamental tradeoff between the number of targets presented and the speed/accuracy. With the 2 target layout we could successfully present 4.3 tps with 86.1% of all targets being correctly predicted. This is a fast pace with a reasonable accuracy, but the task itself is quite simple — it is easy to discriminate between one of two choices. On the other hand, with the 16 target layout we could present 3.5 tps and achieve 38.7% accuracy. This is slightly slower and accuracy is dramatically reduced as well. However, the task is much more difficult as there are now 16 keys to select among. The critical point is that either extreme — fast and accurate on a simple task or slow and inaccurate on a difficult task — would seem less than ideal.

To best encapsulate speed, accuracy, and task difficulty into a single metric, we computed the information transfer rate for each experiment. The best configurations consisted of 8 or 16 targets (6.5 and 6.4 bps, respectively). This value is appreciably less than the peak in Fig. 4 lending credence to the fact that online measurements are necessary to best assess high performance prosthetic systems. Furthermore, given the numbers of neural units that we are using, we believe the system may be reaching a saturation point where

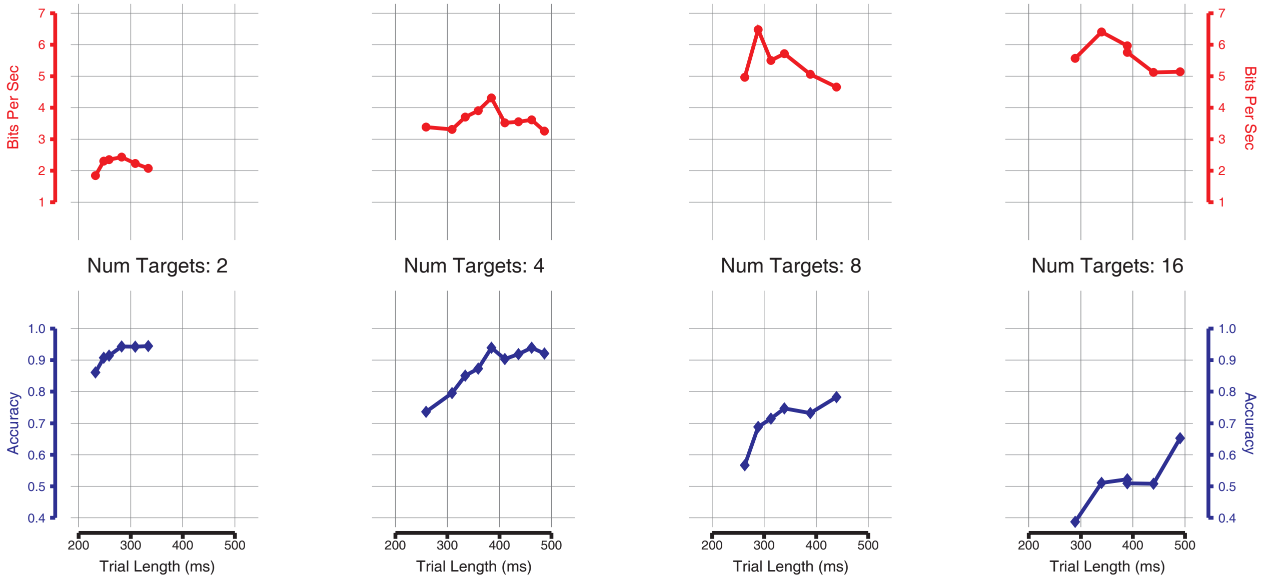

Fig. 5. Accuracy and bps results. Accuracy (bottom row) and bps (top row) are plotted for each target configuration and across varying trial lengths. All results are from monkey H and each data symbol represents online performance calculated from one experiment (many hundreds of trials). Note that within each target configuration, accuracy increases as a function of window length and information transfer rate shows a peak. Across target configurations, average accuracy drops as a function of the number of targets while information transfer rate increases.

adding more targets will not appreciably increase the bit rate of the system. More investigation is needed here.

It is critical to reiterate that our method of calculating tps and bps values is conservative: we use the *entire* trial time which is the sum of T_{skip}, T_{int}, and processing overhead. In other words, our performance numbers are much more representative of the true limits of a clinical system with similar parameters. Had we calculated bps based solely on T_{int} the maximum information transfer rate achieved would have been 28.4 bps with an 8 target configuration and integration time of 50 ms (monkey H).

Finally, we also wished to apply our experimental data to a more predictive setting. As the electrode implant ages, the number of recordable units declines due to reactive immunological processes at the electrode tips. Naturally, overall performance will suffer as a result. Fig. 6(A) shows a contour plot of the performance as a function of the number of units and T_{int}. Losing units results in diminished performance, but by virtue of using delay period activity the drop can be overcome by using longer integration windows. Speed may be compromised but accuracy can be preserved.

Conversely, as electrode technology improves, it may be possible to record many more units than achievable given our current system. With an infinite number of units, how long of an integration window is required to reach 100% accuracy? Or, with an infinite number of units, what is the accuracy of target estimation for a very short integration window? To answer these questions, we fit a curve to the results in Fig. 6(A). Specifically, the following model was fit based on experimentally observed results and population sizes of $\{90,110,130,150\}$:

$$\text{Accuracy} = b_0 * \frac{1}{\text{Number of Units}} + b_1 * \ln(T_{\text{int}}) + b_2$$

The fit was performed using a linear regression and yielded an R^2 value of 0.97. Fig. 6(B) plots simulated data curves as well as the model curve in the limit case of infinite neural units (thick black line). An accuracy of 100% is achievable with 300 ms when there are an infinite number of units. Likewise, with an integration window of 1 ms, the model projects that an infinite number of units can provide an estimation performance of 64%. The fact that plan formation itself may not always be complete by the T_{skip} of 150 ms could be a possible explanation for why an *infinite* number of units cannot provide perfect estimation for small T_{int}.

V. CONCLUSION

We report here the results of a systematic design investigation, encompassing both offline computational simulations and online experimental results, which demonstrate an approximately four fold performance increase (>6 bps vs ∼1.5 bps) beyond the current state of the art. Such performance enhancements should help increase the clinical viability of neurally-controlled communication prostheses. While quantifying neural prosthetic system performance with bps values is becoming more common [15], [17], [23], it has not been routinely reported; this makes direct performance comparison among various neural prosthetic systems difficult. We hope that this study will encourage others in the field to start embracing information transfer rate as a metric for their prosthetic systems.

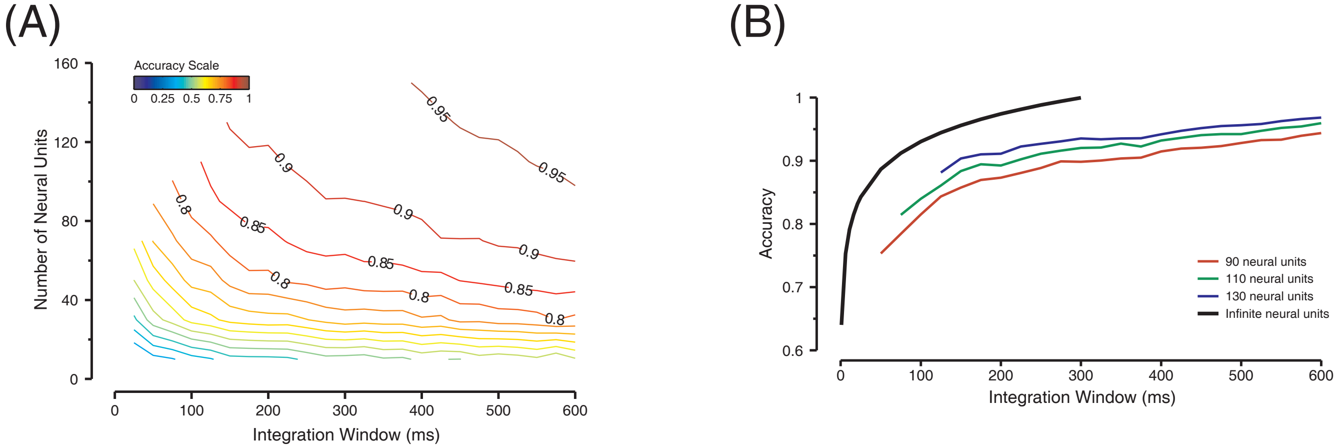

Fig. 6. Performance vs. Numbers of Units. Both plots were generated using data from experiment `H20041118` which involved an 8 target configuration. T_{skip} was fixed at 150 ms. **(A)** Panel shows contours of accuracy as a function of the number of neural units available and T_{int}. The plot was generated by choosing different sized populations of units and sweeping the integration time. For each population size, 100 random subsets of units were drawn (without replacement) from our experimentally recorded population of neural units. Contours are drawn at 5% accuracy intervals. **(B)** Experimentally-observed performance versus window length for three particular population sizes, taken from the same simulation as the left panel. The black curve corresponds to an extrapolated fit for infinite neural units.

ACKNOWLEDGMENTS

We thank Missy Howard for expert surgical assistance and veterinary care. We also thank Drs. Mark Churchland and Maneesh Sahani for valuable assistance during the course of this work.

REFERENCES

[1] E.E. Fetz, "Operant conditioning of cortical unit activity," *Science*, vol. 163, pp. 955–957, 1969.

[2] D.R. Humphrey, E.M. Schmidt, and W.D. Thompson, "Predicting measures of motor performance from multiple cortical spike trains," *Science*, vol. 170, pp. 758–762, 1970.

[3] J.K. Chapin, K.A. Moxon, R.S. Markowitz, and M.A.L. Nicolelis, "Real-time control of a robot arm using simultaneously recorded neurons in the motor cortex," *Nature Neuroscience*, vol. 2, pp. 664–670, 1999.

[4] M.D. Serruya, N.G. Hatsopoulos, L. Paninski, M.R. Fellows, and J.P. Donoghue, "Instant neural control of a movement signal," *Nature*, vol. 416, pp. 141–142, 2002.

[5] D.M. Taylor, S.I. Helms Tillery, and A.B. Schwartz, "Direct cortical control of 3D neuroprosthetic devices," *Science*, vol. 296, pp. 1829–1832, 2002.

[6] J.M. Carmena, M.A. Lebedev, R.E. Crist, J.E. O'Doherty, D.M. Santucci, D.F. Dimitrov, P.G. Patil, C.S. Henriquez, and M.A.L. Nicolelis, "Learning to control a brain-machine interface for reaching and grasping by primates," *PLoS Biology*, vol. 1, pp. 193–208, 2003.

[7] S. Musallam, B.D. Corneil, B. Greger, H. Scherberger, and R.A. Andersen, "Cognitive control signals for neural prosthetics," *Science*, vol. 305, pp. 258–262, 2004.

[8] P.R. Kennedy and R.A.E. Bakay, "Restoration of neural output from a paralyzed patient by a direct brain connection," *NeuroReport*, vol. 9, pp. 1707–1711, 1998.

[9] M.D. Serruya, A.H. Caplan, M. Saleh, D.S. Morris, and J.P. Donoghue, "The braingate pilot trial: Building and testing a novel direct neural output for patients with severe motor impairment.," *Soc. for Neurosci. Abstr.*, 2004.

[10] B. Blankertz, K.-R. Muller, G. Curio, T.M. Vaughan, G. Schalk, J.R. Wolpaw, A. Schlogl, C. Neuper, G. Pfurtscheller, T. Hinterberger, M. Schroder, and N. Birbaumer, "The bci competition 2003: Progress and perspectives in detection and discrimination of eeg single trials," *IEEE Transactions on Biomedical Engineering*, vol. 51, pp. 1044–1051, 2004.

[11] J.R. Wolpaw and D.J. McFarland, "Control of a two-dimensional movement signal by a noninvasive brain-computer interface in humans," *PNAS*, vol. 101, no. 51, pp. 17849–17854, 2004.

[12] E.C. Leuthardt, G. Schalk, J.R. Wolpaw, J.G. Ojemann, and D.W. Morann, "A brain-computer interface using electrocorticographic signals in humans," *Journal of Neural Engineering*, vol. 1, pp. 63–71, 2004.

[13] P.R. Kennedy, R.A.E. Bakay, M.M. Moore, K. Adams, and J. Goldwaithe, "Direct control of a computer from the human central nervous system," *IEEE Transactions on Rehabilitation Engineering*, vol. 8, pp. 198–202, 2000.

[14] P.G. Patil, J.M. Carmena, M.A.L. Nicolelis, and D.A. Turner, "Ensemble recordings of human subcortical neurons as a source of motor control signals for a brain-machine interface," *Neurosurgery*, vol. 55, pp. 27–38, 2004.

[15] D.M. Taylor, S.I. Helms Tillery, and A.B. Schwartz, "Information conveyed through brain-control: cursor vs. robot," *IEEE Transactions on Neural Systems and Rehabilitation Engineering*, vol. 11, pp. 195–199, 2003.

[16] S.I. Ryu, G. Santhanam, B.M. Yu, and K.V. Shenoy, "High speed neural prosthetic icon positioning," *Soc. for Neurosci. Abstr.*, 2004.

[17] G. Santhanam, S.I. Ryu, B.M. Yu, and K.V. Shenoy, "High information transmission rates in a neural prosthetic system," *Soc. for Neurosci. Abstr.*, 2004.

[18] G. Santhanam, M. Sahani, S.I. Ryu, and K.V. Shenoy, "An extensible infrastructure for fully automated spike sorting during online experiments," *Proceedings of the 26th Annual International Conference of the IEEE EMBS, San Francisco, CA*, pp. 4380–4384, 2004.

[19] A.P. Georgopoulos, A.B. Schwartz, and Kettner, "Neuronal population coding of movement direction," *Science*, vol. 233, pp. 1416–1419, 1986.

[20] C.E. Shannon, "A mathematical theory of communication," *Bell System Technical Journal*, vol. 27, pp. 379–423 and 623–656, 1948.

[21] T.M. Cover and J.A. Thomas, *Elements of Information Theory*, John Wiley, New York, 1990.

[22] J. Messier and J.F. Kalaska, "Covariation of primate dorsal premotor cell activity with direction and amplitude during a memorized-delay reaching task," *J Neurophysiol*, vol. 84, pp. 152–165, 2000.

[23] J.R. Wolpaw, N. Birbaumer, W.J. Heetderks, D.J. McFarland DJ, P.H. Peckham, G. Schalk, E Donchin, L.A. Quatrano, C.J. Robinson, and T.M. Vaughan, "Brain-computer interface technology: A review of the first international meeting," *IEEE Transactions of Rehabilitation Engineering*, vol. 8, pp. 164–173, 2000.